IC 225: a dwarf elliptical galaxy with a peculiar blue core

Qiusheng Gu, Yinghe Zhao, Lei Shi, Zhixin Peng and Xinlian Luo

Department of Astronomy, Nanjing University, Nanjing 210093, China

qsgu,yhzhao,xlluo@nju.edu.cn

ABSTRACT

We present the discovery of a peculiar blue core in the elliptical galaxy IC 225 by using images and spectrum from the Sloan Digital Sky Survey (SDSS). The outer parts of the surface brightness profiles of u-, g-, r-, i- and z-band SDSS images for IC 225 are well fitted with an exponential function. The fitting results show that IC 225 follows the same relations between the magnitude, scale length and central surface brightness for dwarf elliptical galaxies. Its absolute blue magnitude (M_B) is $-$ 17.14 mag, all of which suggest that IC 225 is a typical dwarf elliptical galaxy. The g$-$r color profile indicates a very blue core with a radius of 2 arcseconds, which is also clearly seen in the RGB image made of g-, r- and i-band SDSS images. The SDSS optical spectrum exhibits strong and very narrow nebular emission lines. The metal abundances derived by the standard methods, which are 12+log(O/H) = 8.98, log(N/O) = -0.77 and 12+log(S^+/H^+) = 6.76, turn out to be significantly higher than that predicted by the well-known luminosity-metallicity relation. After carefully inspecting the central region of IC 225, we find that there are two distinct nuclei, separated by 1.4 arcseconds, the off-nucleated one is even bluer than the nucleus of IC 225. The asymmetric line profiles of higher-order Balmer lines indicate that the emission lines are bluer shifted relative to the absorption lines, suggesting that the line emission arises from the off-center core, whose nature is a metal-rich HII region. To the best of our knowledge, it is the first high-metallicity HII region detected in a dwarf elliptical galaxy.

Subject headings: Galaxies: elliptical and lenticular, cD — Galaxies: starburst — Galaxies: individual: IC 225

1. Introduction

Dwarf elliptical galaxies, which typically have absolute blue magnitudes fainter than $M_B = -18$ mag, are the most numerous type of galaxies in the local universe. Their formation and evolution have important consequences for both the galaxy luminosity function

and constraints of cosmological models (see the review by Ferguson & Binggeli 1994 and references therein). Recently Graham (2005) suggested that dwarf elliptical galaxies form a continuous extension, both chemically and dynamically, with the more luminous (ordinary) elliptical galaxies (see also Guzman et al. 2003). Bender et al. (1992) proposed that dwarf ellipticals could be bulges of failed disk galaxies which could not acquire material enough to form a significant disk component due to the tidal interaction by a nearby massive galaxy. Alternatively, Gerola et al. (1983) and Mirabel et al. (1992) suggested that dwarf ellipticals form as debris from either the explosion during the initial starburst phase of massive galaxies or giant-galaxy collisions.

IC 225 is a nearby elliptical galaxy in the RC3 catalog (de Vaucouleurs et al. 1991), also detected in both the Markarian (Mrk 1038, Markarian et al. 1977) and KISO (KUG 0223+009, Takase & Miyauchi-Isobe 1986) surveys of galaxies with UV excess. Its redshift is 0.00512 from the Sloan Digital Sky Survey Data Release 2 (SDSS DR2, Abazajian et al. 2004), which corresponds to a distance of 20.6 Mpc (for a Hubble constant of $H_0 = 75$ km s^{-1} Mpc^{-1}, $\Omega_M = 0.3$ and $\Omega_\Lambda = 0.7$), the absolute blue magnitude (M_B) is then estimated to be -17.14 mag. The fact that there is no known companion to this object within 30 arcmin by using the NASA/IPAC Extragalactic Database (NED) suggests that it is most probably isolated. Therefore, it should be classified as an isolated, dwarf elliptical galaxy (dE). Maehara et al. (1987) and Augarde et al. (1994) have shown that its nucleus exhibits emission lines. Based on the emission line ratios, Comte et al. (1994) determined that the line emission is dominated by photoionization from young stars and that the oxygen abundance is [12+log(O/H)] = 8.90. Though the spectrum clearly indicates the presence of recent star-forming activity, it is interesting to note that 21cm HI observations show that there is little HI gas in IC 225 (Thuan et al. 1999; Salzer et al. 2002). Such active star-forming dEs were thought to be rare as they had lost their gas and dust long ago (Mori et al. 1997). However, recently Drinkwater et al. (2001) discovered Hα emission in about 25% of the dEs during the spectroscopic survey of the Fornax cluster (see also Michielsen et al. 2004).

In this paper, we present the imaging and spectroscopic data from the Sloan Digital Sky Survey for the galaxy IC 225, where we detect a compact blue core at the center of IC 225. More interestingly, we find that there are two distinct nuclei in the center of IC 225. The SDSS spectrum exhibits strong and narrow emission lines and is very similar to a metal-rich HII region. This paper is organized as follows: in Section 2 we present the images and optical spectrum for IC 225, both of which are taken out from SDSS. In Section 3 we present the results of surface brightness distributions for five-band SDSS images, we also estimate the star formation rates (SFRs) from Hα and far-infrared luminosities and derive metal abundances for IC 225. Finally we discuss our results in Section 4 and draw

conclusions in Section 5.

2. The Data

The Sloan Digital Sky Survey (SDSS) is the most ambitious astronomical, both photometric and spectroscopic, survey project which has ever been undertaken (Gunn et al. 1998; Blanton et al. 2003). Recently we cross-correlate the SDSS spectroscopic archive data base (Data Release 2; Abazajian et al. 2004) with the Third Reference Catalogue of Bright Galaxies (RC3; de Vaucouleurs et al. 1991), derive a sample of 1049 galaxies available with both morphological classification and spectroscopic information. This sample is large enough to study the circumnuclear star forming activity along the Hubble sequence, which will be presented by Shi et al. (2005).

Here we present the study of low-luminosity elliptical galaxy IC 225 by using SDSS images and spectroscopic data. Figure 1 shows the RGB false-color image of the central 2.0 $\times$ 2.0 arcminutes for IC 225, taken from the SDSS DR3 Finding Chart Tool webpage[1], which combines information from g-, r- and i-band SDSS images by using the algorithm given by Lupton et al. (2004). It is clearly seen that there exists a blue core at the center of IC 225, while the light distribution is very smooth and there is no any sign of bar, spiral arms or any recent interacting remnants and tidal tails.

In Figure 2 we show the SDSS optical spectrum for IC 225. The SDSS fiber size is 3 arcseconds, which corresponds to the diameter of 300pc at the distance of IC 225. We can easily identify strong nebular emission lines, such as Balmer lines (Hα, Hβ and Hγ), [OIII]λ4959,5007, [NII]λ6548,6583 and [SII]λ6716,6732, etc, as already shown by Augarde et al. (1994). Two interesting points are that: 1) all emission lines are very narrow, the full widths at half maximum (FWHM) of Balmer emission lines are just as narrow as those of forbidden lines, such as [OIII] and [SII], which are *only* 170 km s^{-1}; 2) higher-order Balmer absorption lines in the wavelength range of $3800 - 4000$ Å are clearly presented, which have been taken as the unambiguous evidence of intermediate-aged ($\sim 10^8$ yr) stellar populations (Gonzalez Delgado, Leitherer & Heckman 1999).

[1]http://cas.sdss.org/dr3/en/tools/chart/chart.asp

3. Results

3.1. Radial Profiles

It is known that the surface brightness of dwarf elliptical galaxies could be better described by an exponential function (Faber & Lin 1983; Binggeli, Sandange & Tarenghi 1984; Graham & Guzman 2003). In Figure 3 we show the surface brightness distribution for SDSS 5-band (u, g, r, i, and z) images by using the standard tasks in *IRAF* [2].

The central 4-5 arcseconds in IC 225 are clearly affected by the presence of recent active star forming activity (as can be seen in the color profile shown in Fig. 4), we thus only fit the surface brightness profiles beyond 5 arcseconds for all SDSS 5-band images by using both a de Vaucouleurs $R^{1/4}$ and an exponential law. We find that a single exponential law gives a statistically better fit (e.g. the minimum χ^2), whose χ^2 is typically 50% smaller than the fit by the de Vaucouleurs $R^{1/4}$ law. In Fig. 3 we also show the best fits by an exponential law as the solid lines and the fitting results are summarized in Table 1, where we present the scale length (R_S), central surface brightness (μ_0) and the rms values of the fitting. We find that the extrapolated central surface brightness and the scale length for IC 225 obey the same relations between absolute magnitude and central surface brightness/scale length derived for a large sample of dwarf elliptical galaxies (e.g. Fig. 9 Binggeli & Cameron 1991), suggesting that IC 225 is a typical dwarf elliptical galaxy.

After carefully matching PSF profiles of g- and r-band images, we also measure the g−r color distribution for IC 225 in Figure 4. It is very interesting to find that the g−r color is exceptionally bluer in the center 2" region than that of the outer part, just as the blue cores found in the higher redshift elliptical galaxies (Menanteau et al. 2001). In the central region of IC 225, the mean color of g−r is 0.22 mag, while in the outer region, the g−r color distribution is nearly uniform but much redder (0.54 mag). The radial distribution of color (g−r) clearly indicates that the starburst activity in IC 225 is highly concentrated in the central region and also confirms the finding of the blue core in the false-color RGB image.

---

[2]IRAF is distributed by the National Optical Astronomy Observatories, which is operated by the Association of Universities for Research in Astronomy, Inc., under cooperative agreement with the National Science Foundation.

3.2. Star Forming Activity

An important and unavoidable issue in the study of emission-line spectra is the dilution from the underlying old stellar populations, particularly for the Balmer lines. One of popular methods to remove the contribution from old stellar population is to use stellar population synthesis model (Kauffmann et al. 2003; Cid Fernandes et al. 2004; Hao et al. 2005). We use the same stellar population synthesis code, STARLIGHT version 2.0, as Cid Fernandes et al. (2004) to study the stellar properties of IC 225 through fitting the SDSS optical spectrum. The best fit is shown in Figure 5, where we plot the synthetical and pure emission-line (subtracting the best matched model from the observed spectrum) spectra, together with flux- and mass- fractions of 15 different-aged Simple Stellar Populations (SSP) which are chosen from Bruzual & Charlot (2003). The light contributions from young (age $< 10^8$ yr), intermediate-aged ($10^8 \leq$ age $< 10^9$ yr) and old ($\geq 10^9$ yr) stellar components are 40%, 56% and 4%, respectively.

On the other hand, we can also use the equivalent widths (EWs) of the Balmer emission lines to constrain the ages of the underlying (ionizing) stellar populations (e.g. Leitherer & Heckman 1995; Stasińska & Leitherer 1996). For IC 225, the EWs of Hα and Hβ emission lines relative to the continuum due to the young (age $< 10^8$ yr) stellar population alone are 227.5 and 45 Å, respectively, which suggest the age of young starburst to be $6 \sim 7 \times 10^6$ yrs as compared with a Simple Stellar Population model by adopting Salpeter's Initial Mass Function (IMF) with $\alpha = 2.35$ and $M_{up} = 100 M\odot$ at solar metallicity (Stasińska & Leitherer 1996).

From the pure emission-line spectrum, we can measure the accurate fluxes of emission lines as listed in Table 2, the line flux errors are typically less than 5%. Using emission line flux ratios, the so-called BPT diagrams (Baldwin, Phillips & Terlevich 1981; Veilleux & Osterbrock 1987), we confirm that the nebular photoionization in IC 225 is dominated by starburst activity (Comte et al. 1994).

By assuming Case B recombination and a standard reddening law (Cardelli, Clayton & Mathis 1989), we could estimate the nebular extinction from the observed $H\alpha/H\beta$ and $H\gamma/H\beta$ Balmer decrements (see Torres-Peimbert, Peimbert & Fierro 1989), which are

$$A_V^{H\alpha} = 6.60 \times \log(\frac{F_{H\alpha}/F_{H\beta}}{I_{H\alpha}/I_{H\beta}}) \quad (1)$$

$$A_V^{H\gamma} = -16.37 \times \log(\frac{F_{H\gamma}/F_{H\beta}}{I_{H\gamma}/I_{H\beta}}) \quad (2)$$

Where $F_{H\alpha}/F_{H\beta}$,$F_{H\gamma}/F_{H\beta}$ and $I_{H\alpha}/I_{H\beta}$, $I_{H\gamma}/I_{H\beta}$ are the observed and intrinsic Balmer decrements, respectively. In this paper, we adopt the intrinsic ratios of $I_{H\alpha}/I_{H\beta}$ and $I_{H\gamma}/I_{H\beta}$ to be 2.87 and 0.466, respectively (Osterbrock 1989). For IC 225, the observed $F_{H\alpha}/F_{H\beta}$ and $F_{H\gamma}/F_{H\beta}$ (measured from the pure emission line spectrum) is equal to 3.78 and 0.419, then the nebular extinction, $A_V^{H\alpha}$ and $A_V^{H\gamma}$, are estimated to be 0.79 and 0.76 mag, respectively. These two values are nearly the same, which indicates that the stellar population synthesis model is successful to remove the old stellar contribution, the fluxes of emission features are measured accurately and reliably. In the following we will assume the nebular extinction (A_V) to be 0.775 to derive the extinction-corrected fluxes for emission lines.

By using the empirical relation between nebular emission line luminosity and star formation rate (SFR) given by Kennicutt (1998), we can derive the SFR from Hα luminosity. For IC 225, the extinction-corrected Hα luminosity is $L_{\rm H\alpha} = 3.0 \times 10^{39}\ ergs^{-1}$ and the corresponding $\rm SFR_{H\alpha}$ for the central 300 pc in IC 225 is equal to 0.024 M$\odot$ yr^{-1}. At the same time, we could also estimate the SFR from the far infrared (FIR) luminosity (also given by Kennicutt 1998). For IC 225, the IRAS fluxes at 12μm, 25μm, 60μm and 100μm are 0.085, 0.142, 0.192 and 0.477 Jy, respectively, which are taken from the IRAS Faint Source Catalog (Moshir et al. 1989). Thus, the FIR luminosity is equal to 1.55 $\times$ 10^8 L$\odot$ and the corresponding $\rm SFR_{FIR}$ is equal to 0.027 M$\odot$ yr^{-1}, nearly the same as that derived from Hα luminosity. As we know, IRAS aperture size is rather large, typically a few arcminutes. However, the SFR derived from Hα emission could be underestimated because of SDSS aperture effects, which will be addressed in the next Section where we present a detailed description of these effects.

3.3. Metal Abundances

Due to low redshift of IC 225, [OII]λ3727 does not appear in the SDSS spectrum. We find that Augarde et al. (1994) presented the relative intensities of emission lines: [OII]λ3727, Hα, [NII]λ6584 and [SII]λ6725 to Hβ line flux, which are 1.448, 3.804, 0.823, and 1.04, respectively, while our measurements of relative intensities for Hα, [NII]λ6584 and [SII]λ6725 are 3.782, 0.836, and 1.155, respectively. The differences are less than 10%, so we just simply assume [OII]λ3727/Hβ = 1.448 for the further analysis.

Following the standard methods to compute metal abundances (Pagel et al. 1992) and assuming that most of the oxygen is in the first- and second-ionization levels, therefore O/H = (O^++O^{++})/H^+ and N/O = N^+/O^+, the derived ionic abundances are that 12+log(O/H) = 8.98, log(N/O) = -0.77 and 12+log(S^+/H^+) = 6.76, which confirm the oxygen abundance of 8.90 by Comte et al. (1994) and turn out to be significantly higher than solar. By using the

luminosity-metallicity relation for a sample of isolate nearby dwarf galaxies and HII regions (Figure 2 in Duc et al. 2004), for IC 225, M_B = -17.14, the predicted oxygen metallicity is 8.2, which is far smaller than the observed one(8.98), with the maximum difference of 0.78 dex.

We note that the abundance commonly used in the luminosity-metallicity relation of dwarf ellipticals (e.g. Barazza & Binggeli 2002) is the iron abundance in the stars. It is well known that because the iron production has a longer timescale (associated with SN Ia) than the oxygen (associated with SN II) an overabundance of oxygen with respect to iron is commonly found in the stellar spectra of elliptical galaxies (Thomas et al. 2002). This overabundance is expected to be even more significant when comparing iron in the stars with the oxygen in the ISM. Therefore, it might be possible that although the oxygen abundance of the ISM is slightly above solar, the iron abundance in the stars is not as different from that found in dwarf ellipticals of similar luminosity. Note, however, that the O/Fe overabundance seems to be smaller in low luminosity ellipticals than in massive ones. In the case of IC225, the low S/N for iron absorption lines hampers us for estimating the iron abundance. Using the empirical calibration for the mean (universal) luminosity − metallicity relation given by Barazza & Binggeli (2002), we predict the iron abundance [Fe/H] for IC 225 to be -0.65.

4. Discussion

We have shown that for IC 225 the absolute blue magnitude is − 17.14 mag, the outer parts of surface brightness distributions are well fitted by an exponential law, and the fitting results show that IC 225 follows the same relations between the magnitude and the scale length and central surface brightness for dwarf elliptical galaxies, all of which suggest that IC 225 is a typical dwarf elliptical galaxy (Binggeli 1994; Kormendy & Bender 1994). However, several observational evidences, such as strong but narrow nebular emission lines, the blue core in the RGB image, blue g−r color in the central 2" region, support that the young star-forming activity is occurring at the nuclear region.

We search in the view field of 30 arcminutes of IC 225 by using the NASA/IPAC Extragalactic Database (NED), and don't detect any interacting companion. But when we check the SDSS images carefully, we find that there are two distinct nuclei, separated by 1.4 arcseconds in the central region of IC 225, which is shown in Fig. 6. The off-nucleated core has very blue (g−r) color, even bluer than the nucleus of the galaxy; it almost disappears in the i-band but it has higher surface brightness than the nucleus in the u-band image. Could it be a dwarf galaxy or a halo cluster swallowed by IC225 and thus trigger the starburst activity in IC 225 ? The high metallicity (12+log(O/H)=8.98) rules out such possibility of

a dwarf galaxy or a halo cluster, which is used to be metal-poor (1/10 solar or even less). However, we still can't have a direct answer due to the no spatially-resolved information from the SDSS spectrum, but we can have a try to probe its nature by measuring the recession velocity of both several emission lines and absorptions lines, looking for a velocity difference that could indicate that while the absorption comes in the most part from stars in the high-surface brightness nucleus, the emission probably arises from an off-nuclear HII region with slightly different radial velocity and by using the well-known luminosity-metallicity relation (Duc et al. 2004; Tremonti et al. 2004).

In order to make sure that the off-nuclear core is physically associated with IC 225 and is the place where the line emission arises from, we try the following ways. First, we find that the off-nucleated region in the u-band image is spatially more extended than the PSF profile that excluded a QSO as the background source or a field star as the foreground source. Second, we have measured the aperture color of the nucleus and off-nuclear region. After carefully checking the PSF profiles of g- and r-band images, we smooth the g-band image by convolving a Gaussian kernel to match the r-band PSF. By using tasks of *geomap* and *geotran* in IRAF, we rotate and shift the g-band image relative to the r-band image so that we could accurately measure the aperture colors (g−r) of the nucleus and the off-nuclear region with aperture size of 1.5 pixels, which are 0.23 and 0.20 mag, respectively, and quantitatively confirm that the off-nuclear region is even bluer than the nucleus of IC225. Third, fortunately the SDSS spectrum of IC 225 shows higher-order Balmer absorption lines so that we can compare the recession velocities of both Balmer emission lines and absorption lines. As shown in the inset of Fig. 2, higher-order Balmer emission lines (such as H_9, H_8, Hϵ and Hδ) are clearly present in the centers of absorption lines and these emission-absorption line profiles are all asymmetric, the red wings are more deeper than the blue wings, which suggests that the emission lines are bluer shifted relative to the absorption lines. Quantitatively we use the task *specfit* in IRAF to fit the profiles of Hϵ and Hδ (as shown in Fig. 7), and confirm that the centroids of emission lines are bluer shifted by 0.4 and 0.5 Å relative to the absorption lines, respectively, suggesting that while the absorption comes in the most part from stars in the high-surface brightness nucleus the emission probably arises from an off-nuclear HII region with slightly different radial velocity. To the best of our knowledge, it is the first high-metallicity HII region detected in a dwarf elliptical galaxy. A similar metal-rich HII region is detected in the spiral galaxy NGC 1232 by Castellanos, Diaz & Terlevich (2002), whose metal abundances are 12+log(O/H) = 8.95, log(N/O) = -0.81 and 12+log(S^+/H^+) = 6.67.

In order to unambiguously understand the nature of these two cores, their relation and the origin of star-forming activity in the central region of IC 225, we need further observational data. Such long-slit optical spectroscopy for this galaxy is under consideration.

Finally, since the size of the SDSS fiber (1.5" in radius) is comparable to the distance between the two regions identified near the center of IC 225, the actual positioning of the fiber is critical for our conclusions about star forming activity in IC 225. For the SDSS, the centroid of an object is defined as the first moment of the light distribution, the r CCDs are served as the astrometric reference CCDs and the relative astrometric accuracy between the r filter and each of the other filters (u, g, i, z) is about 25−35 mas (rms). Pier et al. (2003) have described the astrometric calibration and centroiding algorithm in detail and also estimated centroiding errors for galaxies, ranging from about 60 mas at r $\sim$ 17 mag to 170 mas at r $\sim$ 22 mag, which are independent of seeing. Since it is the r-band image which was used to determine where the fiber should be placed and the nominal coordinates of the fiber center, for IC 225 a significant part of the emission from the off-nuclear region was missing, thus it will lead to underestimate the total SFR from the Hα luminosity detected within the fiber.

5. Conclusions

In this paper, we present new imaging and spectroscopic data for IC 225 from the Sloan Digital Sky Survey (SDSS). The outer parts (beyond 5") of surface brightness distributions of u-, g-, r-, i- and z-band SDSS images for IC 225 are well fitted with an exponential function, the fitting results show that IC 225 follows the same relations between the magnitude, scale length and central surface brightness for dwarf elliptical galaxies, and its absolute blue magnitude (M_B) is − 17.14 mag, suggesting that IC 225 is a typical dwarf elliptical galaxy. However, the SDSS optical spectrum exhibits strong and very narrow nebular emission lines, the RGB image and g−r color distribution indicate a blue core in the central region of IC 225, where we find there exist two distinct nuclei, separated by 1.4 arcseconds, the off-nucleated core is even bluer than the nucleus of the galaxy. From the SDSS spectrum, we derive the oxygen abundance is significantly higher than that predicted by the metallicity-luminosity relation. At the same time, the asymmetric line profiles of higher-order Balmer lines indicate that the emission lines are bluer shifted relative to the absorption lines, which supports that the line emission comes from the off-center region, we thus propose that the off-nucleated core is a metal-rich HII region, which is the first high metallicity HII region known in the dwarf elliptical galaxies. The discovery of a metal-rich HII region in a dwarf elliptical galaxy will provide important clues for the understanding of the star formation history and chemical evolution of dwarf galaxies and of the luminosity-metallicity relation.

The authors are very grateful to the anonymous referee for his/her careful reading of the manuscript and thoughtful and instructive comments which significantly improved the

content of the paper. We would like to thank Jorge Melnick and Jiasheng Huang for valuable discussions and suggestions as well as Roberto Cid Fernandes for sending us the updated code for stellar population synthesis. This work is supported by the National Natural Science Foundation of China under grant 10221001 and the National Key Basic Research Science Foundation (NKBRSG19990754). Funding for the creation and distribution of the SDSS Archive has been provided by the Alfred P. Sloan Foundation, the Participating Institutions, the National Aeronautics and Space Administration, the National Science Foundation, the U.S. Department of Energy, the Japanese Monbukagakusho, and the Max Planck Society. The SDSS web site is http://www.sdss.org/. The SDSS is managed by the Astrophysical Research Consortium (ARC) for the Participating Institutions. The Participating Institutions are The University of Chicago, Fermilab, the Institute for Advanced Study, the Japan Participation Group, The Johns Hopkins University, Los Alamos National Laboratory, the Max-Planck-Institute for Astronomy (MPIA), the Max-Planck-Institute for Astrophysics (MPA), New Mexico State University, University of Pittsburgh, Princeton University, the United States Naval Observatory, and the University of Washington. This research has made use of the NASA/IPAC Extragalactic Database (NED) which is operated by the Jet Propulsion Laboratory, California Institute of Technology, under contract with the National Aeronautics and Space Administration.

REFERENCES

Abazajian K., Adelman-McCarthy J. K., Agueros M. A., et al. 2004, AJ, 128, 502

Augarde R., Chalabaev A., Comte G., Kunth D., Maehara H. 1994, A&AS, 104, 259

Baldwin, J. A., Philips, M. M., & Terlevich, R. 1981, PASP, 93, 5

Barazza F. D., Binggeli B. 2002, A&A, 394, L15

Bender R., Burstein D., Faber S.M. 1992, ApJ, 399, 462

Binggeli, B., Sandage A. & Tarenghi M., 1984, AJ, 89, 64

Binggeli, B. 1994, in ESO/OHP Workshop on Dwarf Galaxies, ed. G. Meylan & P. Prugniel (Garching: ESO), 13

Binggeli B., Cameron L.M. 1991, A&A, 252, 27

Blanton, et al. 2003, AJ, 125, 2276

Bruzual, G., & Charlot, S. 2003, MNRAS, 344, 1000

Cardelli, J. A., Clayton, G. C., & Mathis, J. S. 1989, ApJ, 345, 245

Castellanos M., Diaz A. I., Terlevich E. 2002, MNRAS, 329, 315

Cid Fernandes, R., Gu, Q., Melnick, J. et al., 2004, MNRAS, 355, 273

Comte G., Augarde R., Chalabaev A., Kunth D., Maehara H. 1994, A&A, 285, 1

de Vaucouleurs, G. 1953, MNRAS, 113, 134

de Vaucouleurs, G., de Vaucouleurs, A., Corwin, H.G., Buta, R.J., Paturel, G., & Fouque, P. 1991, Springer-Verlag: New York, Third Reference Catalogue of Bright Galaxies (RC3)

Drinkwater M.J., Gregg M.D., Holman B.A., Brown M.J.I. 2001, MNRAS, 326, 1076

Duc P. A., Bournaud F. Masset F.S. 2004, IAUS217, 550

Faber S.M. & Lin D.M.C., 1983, ApJ, 266, L17

Ferguson H. C., Binggeli B. 1994, A&ARv, 6, 67

Gerola H., Carnevali P., Salpeter E. E. 1983, ApJ, 268, L75

Gonzalez Delgado, R., Leitherer, C., & Heckman, T. 1999, ApJS, 125, 489

Graham A. W. & Guzman R., 2003, AJ, 125, 2936

Graham A. W. 2005, in IAUC 198 on Near-Field Cosmology with Dwarf Elliptical Galaxies, eds. H. Jerjen & B. Binggeli, in press (astro-ph/0505429)

Gunn, J. E., et al. 1998, AJ, 116, 3040

Guzman R., Ostlin G., Kunth D., Bershady M.A., Koo D. C., Pahre M.A. 2003, ApJ, 586, L45

Hao L., et al. 2005, AJ, 129, 1783

Kauffmann G., et al. 2003, MNRAS, 341, 33

Kormendy, J., Bender, R. 1994, in ESO/OHP Workshop on Dwarf Galaxies, ed. G. Meylan & P. Prugniel (Garching: ESO), 161

Kennicutt, R. C. Jr. 1998, ARA&A, 36, 189

Leitherer, C., & Heckman, T. 1995, ApJS, 96, 9

Lupton R., Blanton M.R., Fekete G., et al. 2004, PASP, 116, 133

Maehara H., Noguchi T., Takase B., Handa T., 1987, PASJ, 39, 393

Markarian, B. E.; Lipovetskii, V. A.; Stepanian, D. A.1977, Afz, 13, 397

Menanteau, F., Abraham, R. G., & Ellis, R. S. 2001, MNRAS, 322, 1

Michielsen D., De Rijcke S., Zeilinger W.W., et al. 2004, MNRAS, 353, 1293

Mirabel I.F., Dottori H., Lutz D. 1992, A&A, 256, L19

Mori M., Yoshii Y., Tsujimoto T., Nomoto K., 1997, ApJ, 479, L21

Moshir, M., Copan, G., Conrow, T., et al. 1989, IRAS Faint Source Catalog, IPAC.

Osterbrock, D. E. 1989, Astrophysics of Gaseous Nebulae and Active Galactic Nuclei (Mill Valley: University Science Books)

Pagel B. E. J.; Simonson, E. A.; Terlevich, R. J.; Edmunds, M. G., 1992, MNRAS, 255, 325

Pier J. R., Munn J. A., Hindsley R. B., et al. 2003, AJ, 125, 1559

Salzer J. J., Rosenberg J. L., Weisstein E. W., Mazzarella J. M., Bothun G.D. 2002, AJ, 124, 191

Shi L., Gu Q.S., Zhao Y., et al. 2005, in preparation

Stasińska, G., & Leitherer, C. 1996, ApJS, 107, 661

Takase B. , Miyauchi-Isobe N. 1986, AnTok, 21, 127

Thuan T.X., Lipovetsky V.A., Martin J.M, Pustilnik S.A. 1999, A&AS, 139, 1

Thomas D., Maraston C., Bender R., 2002, Ap&SS, 281, 371

Torres-Peimbert, S., Peimbert, M., & Fierro, J. 1989, ApJ, 345, 186

Tremonti C. A., et al. 2004, ApJ, 613, 898

Veilleux, S., & Osterbrock, D.E. 1987, ApJS, 63, 295

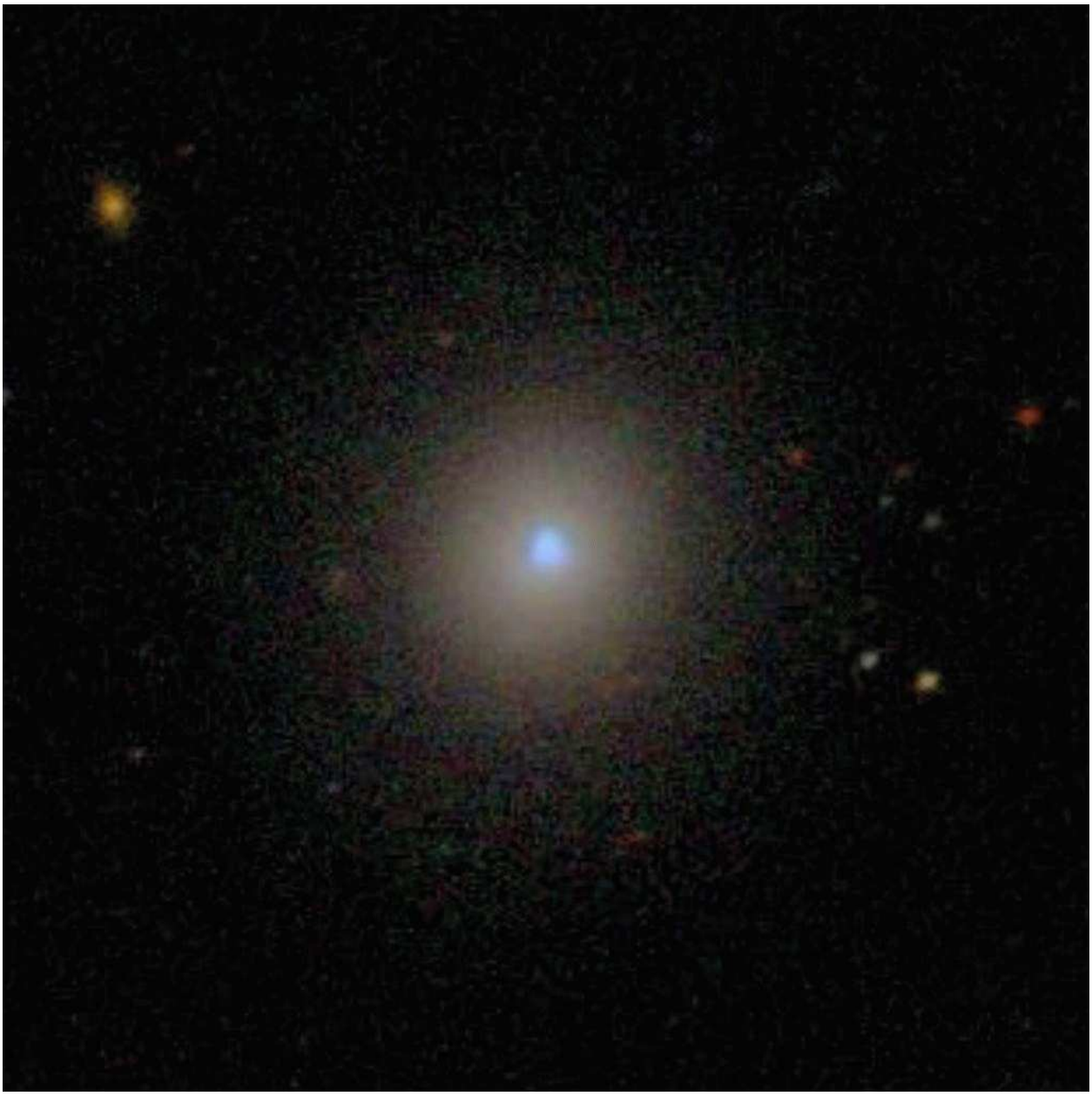

Fig. 1.— The RGB false-color image of IC 225, which combines g-, r- and i-band images from the Sloan Digital Sky Survey. A blue core is seen in the central region. The image size is 2.0 × 2.0 arcminutes.

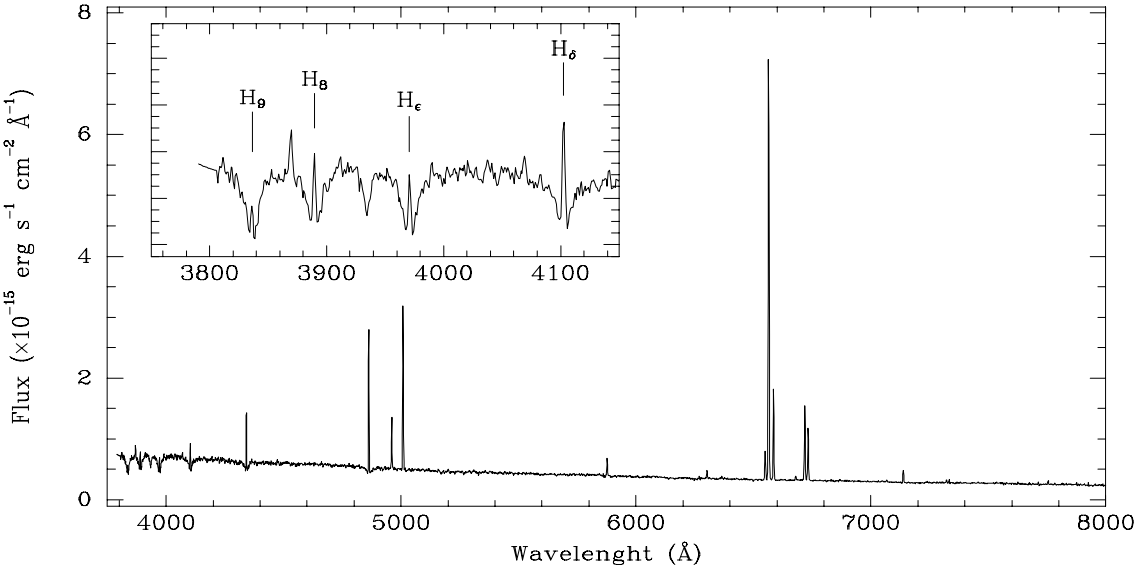

Fig. 2.— The optical spectrum of IC 225, taken from the Sloan Digital Sky Survey. The inset shows enlargement of the wavelength range of 3750 - 4150 Å, where the higher-order Balmer absorption lines are clearly detected and these emission-absorption line profiles are all asymmetric.

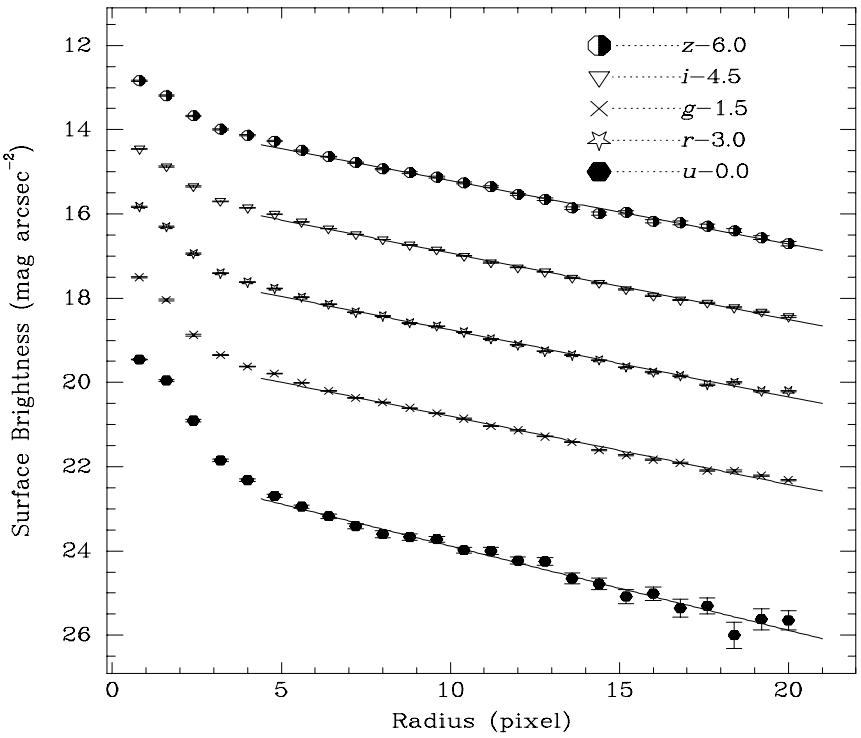

Fig. 3.— Surface brightness of IC 225 as a function of radius for SDSS u-, g-, r-, i, and z-bands images. The solid lines are the best fits with an exponential law only for the outer parts of the surface brightness profiles. The profiles have been shifted for clarity, error bars are also shown for each measured point.

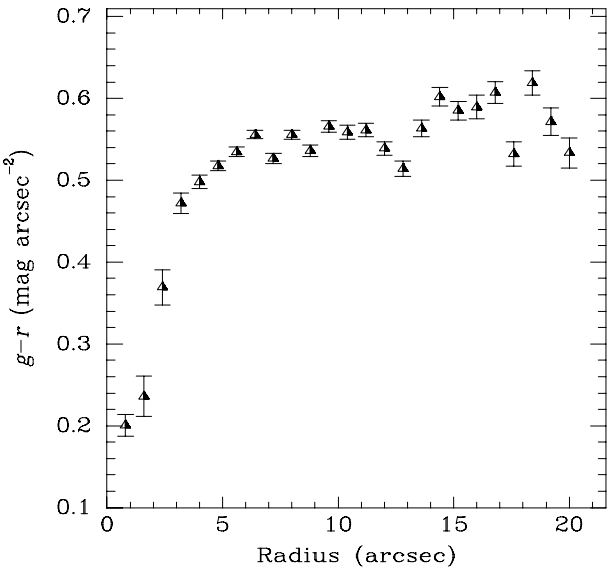

Fig. 4.— The g−r color distribution for IC 225.

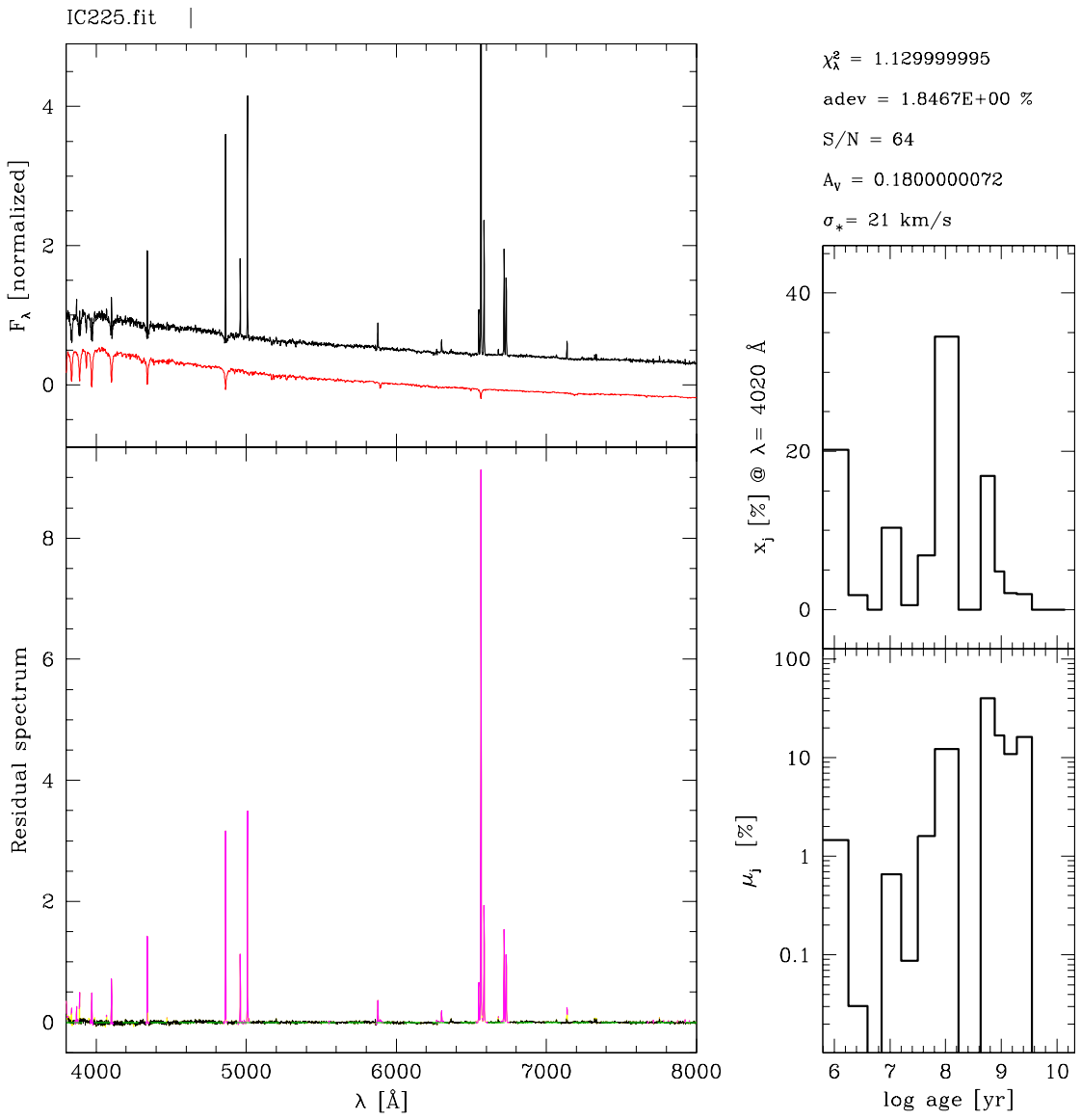

Fig. 5.— Results of the spectral fitting for IC 225. The top left panel shows the logarithm of the observed and the synthetic spectra, which is shown in red color and has been shifted by -0.5 for clarity. The $F_\lambda^O - F_\lambda^M$ residual spectrum is shown in the bottom left panel. Spectral regions actually used in the synthesis are plotted with black color, while masked regions are plotted with the color of magenta. Panels in the right show the population vector binned in the 15 ages of the base. The top panel corresponds to the population vector in flux fraction, normalized to $\lambda_0 = 4540$ Å, while the corresponding mass fractions vector is shown in the bottom.

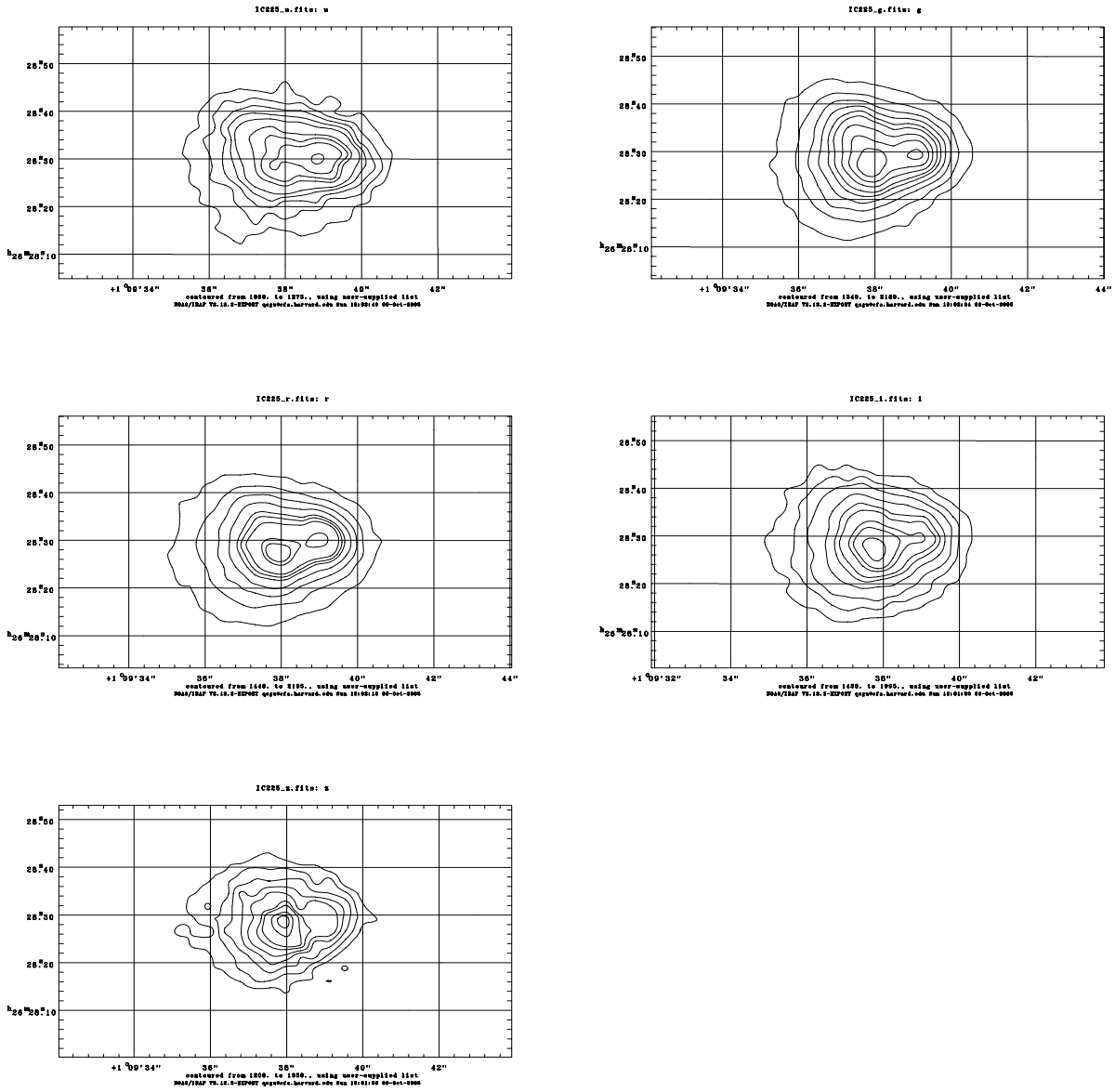

Fig. 6.— The u-, g-, r-, i- and z-band contour plots for the central region of IC 225. Two distinct nuclei are unambiguously found, the off-nucleated core is even bluer than the nucleus of the galaxy, which has higher surface brightness in the u-band but almost disappears in the i-band image.

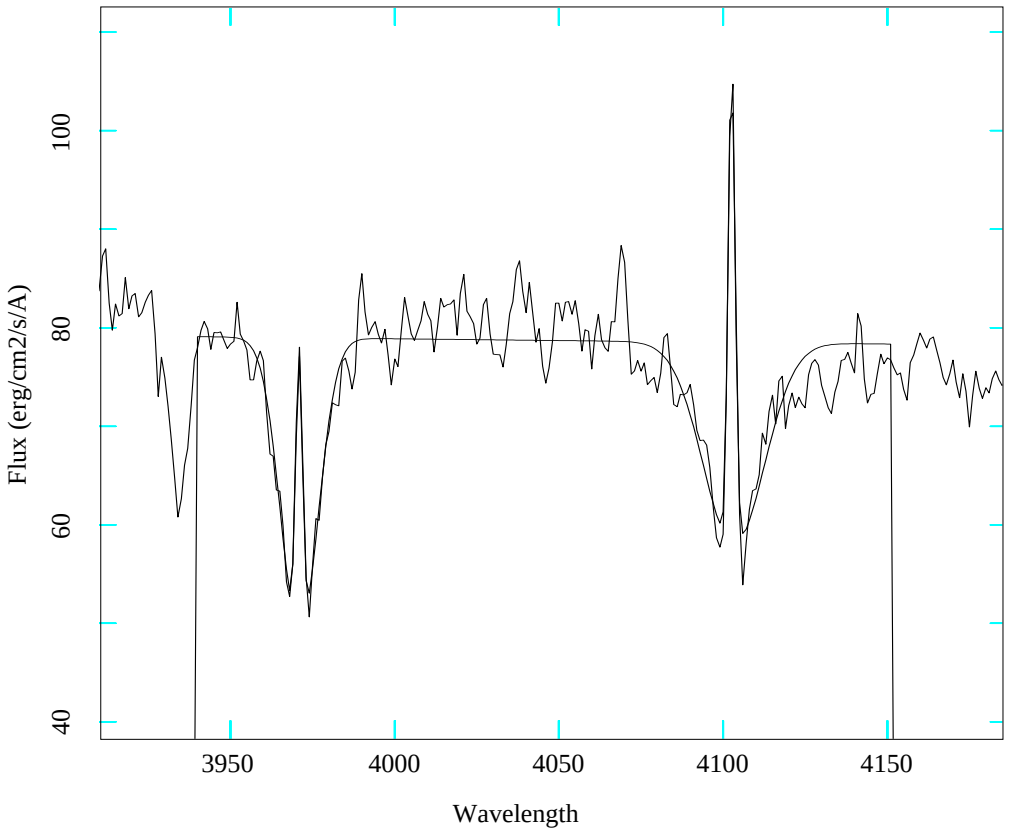

Fig. 7.— The spectral fitting to the absorption+emission line profiles of Hϵ and Hδ. The flux is in unit of $10^{-17} erg cm^{-2} s^{-1} \mathring{A}^{-1}$.

Table 1: Results of fitting the outer parts of surface brightness distribution with an exponential law.

Band	R_S	μ_0	rms
	arcsec	mag/arcsec^2	
u	5.43 ± 0.26	21.89 ± 0.13	0.15
g	6.72 ± 0.14	20.69 ± 0.05	0.05
r	6.84 ± 0.15	20.17 ± 0.05	0.05
i	6.90 ± 0.09	19.86 ± 0.03	0.03
z	7.21 ± 0.16	19.70 ± 0.05	0.05

Table 2: Emission lines properties for IC 225.

Wavelength (Å)	Ion	flux[a]
3835	H9	28.9
3889	H8	96.4
3970	Hϵ	120.2
4101	Hδ	164.8
4340	Hγ	361.2
4363	[O III]	12.2
4861	Hβ	862.6
4959	[O III]	331.5
5007	[O III]	994.6
6300	[O I]	90.2
6548	[N II]	240.3
6563	Hα	3262.3
6583	[N II]	720.9
6716	[S II]	577.5
6732	[S II]	420.1

[a]fluxes are in units of 10^{-17} erg s^{-1} cm^{-2}